

Fermi National Accelerator Laboratory

FERMILAB-Conf-95/086

Review of Calorimetry in Fermilab Fixed-Target Experiments

Michael B. Crisler

*Fermi National Accelerator Laboratory
P.O. Box 500, Batavia, Illinois 60510*

April 1995

Presented at the *1994 Beijing Calorimetry Symposium*, Beijing, China, October 25-27, 1994

Disclaimer

This report was prepared as an account of work sponsored by an agency of the United States Government. Neither the United States Government nor any agency thereof, nor any of their employees, makes any warranty, express or implied, or assumes any legal liability or responsibility for the accuracy, completeness, or usefulness of any information, apparatus, product, or process disclosed, or represents that its use would not infringe privately owned rights. Reference herein to any specific commercial product, process, or service by trade name, trademark, manufacturer, or otherwise, does not necessarily constitute or imply its endorsement, recommendation, or favoring by the United States Government or any agency thereof. The views and opinions of authors expressed herein do not necessarily state or reflect those of the United States Government or any agency thereof.

Review of Calorimetry in Fermilab Fixed-Target Experiments

Michael B. Crisler
Fermi National Accelerator Laboratory
P.O. Box 500, Batavia, IL 60510 USA

The fixed-target program at Fermilab comprises as many as thirteen simultaneous experiments in ten separate beamlines using beams of primary protons, pions, kaons, electrons, neutrinos, and muons. The fixed target beamlines were last in operation in the latter half of 1991, shutting down in 1992. The next fixed target run is scheduled for early 1996. This article describes some of the wide variety of calorimetric devices that were in use in the past run or to be used in the coming run. Special attention is devoted to the new devices currently under construction.

1. CRYSTAL CALORIMETRY

1.1. The KTeV CsI Calorimeter

The KTeV program at Fermilab[1] comprises two experiments, E-832 and E-799. E-832 has the objective of measuring the direct CP violation parameter ϵ'/ϵ to an accuracy of 10^{-4} , and is a follow on to the earlier E-731 measurement[2]. E-799 is also a CP violation experiment and is aimed at detecting the decay $K_L^0 \rightarrow \pi^0 e^+ e^-$ as well as a host of other rare decay modes of the K_L^0 . The most demanding requirements on the KTeV calorimetry come from E-832.

The determination of ϵ'/ϵ requires measurement of the decay rates of K^0 and \bar{K}^0 into $\pi^+\pi^-$ and $\pi^0\pi^0$ final states. The $\pi^+\pi^-$ final states are reconstructed using a conventional magnetic spectrometer. The reconstruction of the $\pi^0\pi^0$ events is accomplished by registering the resulting four photons in the electromagnetic calorimeter. An excellent understanding of the relative acceptance and energy scale of these two classes of events is crucial to the technique, and here the Z vertex resolution for the neutral events plays an important role. It is this consideration that drives the stringent energy and position resolution requirements on the electromagnetic calorimetry. In order to attain the necessary precision in ϵ'/ϵ , the calorimeter resolution must be less than 1% in energy and less than 1 mm in position for the average photon energy of 15 GeV. The dynamic range of the experiment extends to 80 GeV for a single photon, and requires a digitization least count of 2 MeV.

These energy and position resolution require-

ments lead naturally to the selection of a high light output crystal array for the electromagnetic calorimeter. Pure CsI was chosen from among the other candidate materials because it provides a balance of signal speed, spatial uniformity, radiation hardness, and cost which meets the requirements of the experiment. GEANT simulations were used to investigate the effect of crystal granularity and thickness on the ultimate performance of the device. Based on these simulations and on test beam data, a two meter square array of 27 radiation length (50 cm) crystals was selected. The KTeV CsI array is illustrated in Figure 1. The inner one meter square array consists of 2.5 cm square crystals. To reduce the total channel count, the outer perimeter of the array is formed from 5.0 cm square crystals. 15×15 cm² holes are provided for two kaon beams to pass through the calorimeter. The complete array consists of 3100 individual CsI Crystals.

1.1.1. Virtues and Drawbacks of Pure CsI for Electromagnetic Calorimetry

Although pure CsI is well suited to the KTeV calorimetry application, it is not a perfect material. The properties of pure CsI lead to technical challenges that must be addressed in the design of the device. The relevant technical issues are these:

light output: In the configuration required by KTeV, pure CsI crystals typically yield greater than twenty photoelectrons per MeV of deposited energy. This is more than enough to attain the required energy resolution, and results in over 10^6 photoelectrons at the high end of the experi-

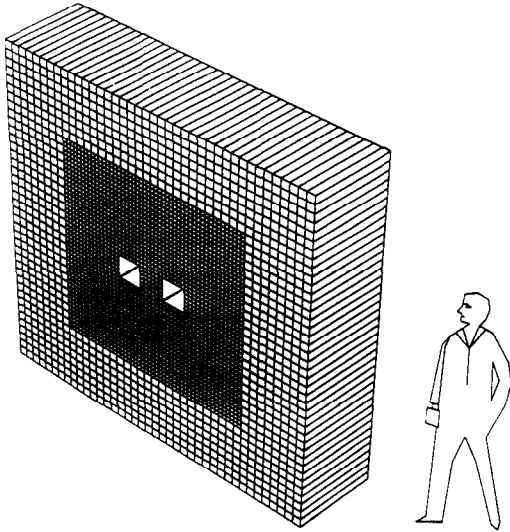


Figure 1. The KTeV CsI Calorimeter Array.

ment's dynamic range. This light level is not sufficient for the use of a photodiode readout, but is quite large for a conventional photomultiplier since the gain is required to be rather low ($< 10^4$). In order to attain the linearity requirements of the experiment at this low gain, a custom photomultiplier tube was developed by Hamamatsu which uses only five stages.

radiation hardness: Estimates of the beam halo suggest that the crystals near the beam hole region will receive as much as 10 kRad of radiation dose during the KTeV experimental program. While pure CsI is nominally very radiation hard, the actual hardness varies from batch to batch and between manufacturers. In order to deal with this problem, the radiation hardness is measured for test samples from each batch of CsI. Tests have shown that the radiation hardness of the final machined crystals correlates well with that of the test samples. Crystals that are thus known to be most radiation hard will be deployed in the high radiation areas around the beam holes. Other less radiation hard crystals will be relegated to the perimeter of the array.

timing characteristics: Compared to the doped CsI crystals that have been used in a number of previous applications, pure CsI is quite fast having a 15 to 25 ns decay constant for the fast component of the light. There is however a significant slow component of the scintillation light having a decay constant from 1 to several microseconds. This slow component results in a rate dependent baseline shift for the device which must be dealt with in the readout.

humidity and temperature dependence: CsI is mildly hygroscopic and must therefore be stored and handled in a dry environment. In addition, the temperature dependence of the scintillation light output of CsI has been measured[3] to be $-1.5\%/^{\circ}C$. This requires that the array be maintained in a temperature and humidity controlled box.

1.1.2. Uniformity and Radiation Hardness

A crucial issue in the performance of a crystal calorimeter is uniformity of response over the volume of the crystal. The spatial fluctuations in the development of an electromagnetic shower coupled with the spatial variations in the response of the device contribute to the resolution. In addition, since the average shower position changes with particle energy, a spatial non-uniformity in the crystals may result in a device with non-linear response. This issue has been analyzed using GEANT simulations with the result that the response of a crystal can vary by no more than 5% from front to back for this contribution to the resolution to be unimportant. While this uniformity specification is not satisfied by bare CsI crystals, it has been shown that differential wrapping (part of the crystal wrapped with black material, part wrapped with reflective material) can be used to bring typical crystals into conformity with the specification. In the KTeV device, individual crystals will be wrapped in 1 mil polyethylene which is either black coated or aluminized (or in some cases aluminized and partially masked with stripes which are ink applied with a pen).

An additional complication arises due to the manufacture of the crystals. When the first orders for KTeV CsI crystals were placed, no manufacturer had been able to produce a 50 cm long

crystal that met the uniformity requirements. Continuous 50 cm crystals were successfully produced only after the first round of crystal procurement. Consequently, only 20% of the KTeV array will consist of continuous 50 cm crystals. The remaining 80% of the array will be formed from 25 cm pieces glued together to form the required 50 cm length. The pieces are glued before machining, so there is not a problem for mechanical tolerances. The glue joint does however produce a response step which must be compensated in the wrapping process. The required 5% uniformity can be attained if the non-uniformity of the bare crystal doesn't exceed 30% over its length, and this has been selected as the manufacturing specification for the crystals, including the effect of the glue joint.

Radiation hardness is also a uniformity issue. If a crystal is radiation damaged, then its spatial uniformity will be altered. Crystals that originally met specifications will then fail and the resolution and linearity will deteriorate. This issue has been studied in detail by measuring the response as a function of position for crystals before and after a radiation dose. The measured response is then fed into a Monte Carlo calculation using simulated shower fluctuations. Figure 2 shows the effect of irradiation on a radiation sensitive CsI crystal. The response, normalized to the response near the PMT, develops a steeper slope, and after 8 kRad, the resolution has deteriorated by nearly a factor of two. Figure 3 shows a radiation hard crystal which is able to absorb 8 kRad and remain within specs. In order to keep the KTeV device within specifications for the duration of the program, it is necessary that about 10% of the crystals be radiation hard to the 10 kRad level.

1.1.3. Light Detection and Digitization

Because of the slow component of the CsI scintillation light, the KTeV calorimeter readout must provide baseline information in addition to the measurement of the signals. The other more traditional problem encountered in transducing the light from an electromagnetic calorimeter is maintaining the required linearity over a very large dynamic range. When using photomulti-

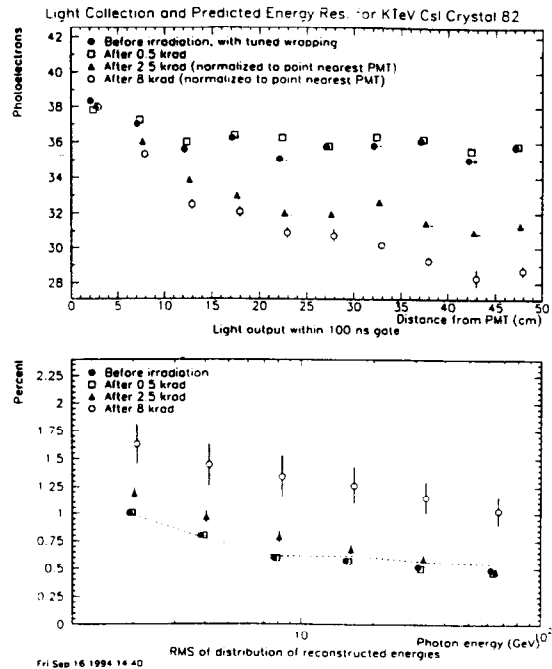


Figure 2. The effect of rad damage on a radiation sensitive CsI crystal.

plier readout, the dynamic range is limited at the high end by the onset of PMT non-linearity due to the space charge effect. The low end of the dynamic range is determined by the noise level in the digitization electronics. In the KTeV application, the dynamic range specification is set by a requirement for 2 MeV least count and a high end sensitivity of 80 GeV. The problem is exacerbated by the small cell size of the device which forces the use of 3/4" diameter PMT's which are significantly more sensitive to space charge saturation than larger PMT's.

In order to maximize the linear range, a custom photomultiplier tube was developed by the Hamamatsu corporation which employs five stages with a mesh anode. The anode lies between the fourth and fifth stages, and the largest part of the gain occurs in the last stage. This results in linearity up to 30 mA instantaneous anode current. Although this is significantly better performance

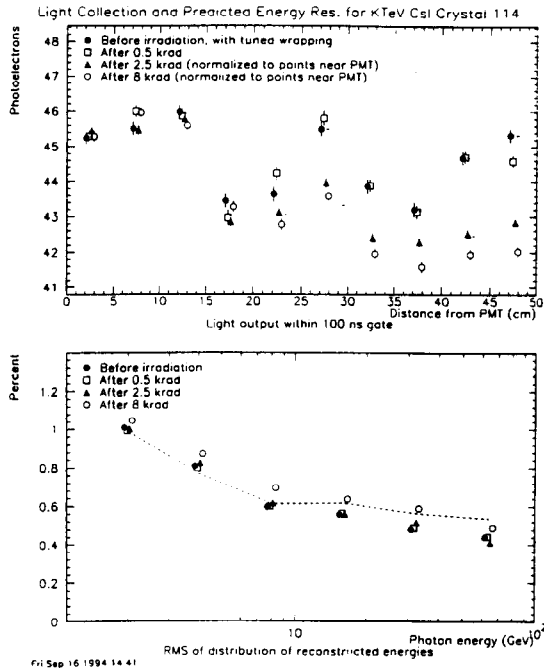


Figure 3. The effect of rad damage on a more robust CsI crystal.

than is typical of 3/4" diameter PMT's, it is not sufficient for attaining the KTeV dynamic range specification with a conventional ADC, since the noise performance would still need to be better than a few fCoul per count.

The noise threshold and baseline measurement requirements of KTeV are handled nicely by a technology that was developed for the SDC calorimeter. The "Digital PMT" technology[4] is a deadtimeless 53MHz flash digitizer with a 17 bit dynamic range. The heart of the device is a custom integrated circuit which splits the PMT anode current into binary ranges (1/2, 1/4, 1/8 etc). Each of these current streams is sampled by an independent four-capacitor deadtimeless, integrating sample-and-hold circuit. During any 19 ns clock cycle, the current is charging one of the four capacitors, while the second capacitor is settling, the third is available to a multiplexer, and the fourth is being cleared. With each clock

tic, the roles of the four capacitors are permuted. A freshly cleared capacitor is always available to integrate the next sample, thus attaining dead-timeless operation. Two clock ticks after integration, the settled capacitor from each of the nine ranges is presented to the multiplexer which determines which capacitor voltage is "on scale" and passes that voltage to the output, along with ID bits to identify which range was selected. The output of the current splitter chip is then presented to a commercial 8-bit flash digitizer. The 8-bit data from the flash plus the range information provide the full 17-bit dynamic range of the system. The entire digitization circuit is connected directly to the base of the PMT without delay cables resulting in excellent low end noise performance of less than 5 fCoul per count.

The resulting system satisfies the dynamic range and baseline measurement requirements of the KTeV experiment, and provides the additional bonus of a complete measurement of the pulse shape. This may ultimately prove to be a powerful tool when used to analyze accidental energy pileup effects.

1.1.4. Mechanical Considerations

Because of the temperature dependence of the CsI light output, it is crucial to maintain the temperature of the array constant to a fraction of a degree. This problem is especially challenging due to the proximity of the PMT voltage dividers and the digitization electronics to the array. The power output of these devices is approximately 3 watts per channel resulting in a total heat load of 9kW at the back of the array. In order to maintain the required temperature stability of the array, the power dissipating components of the PMT divider and the digitization electronics are physically separated from the back of the array by a gap of 15 cm. The PMT bases consist of an upstream piece which attaches to the PMT and a downstream piece containing the voltage divider and the digitizer. The upstream and downstream pieces are joined by an umbilical of cables which carry the cathode and dynode voltages and the anode signal. So that the high frequency behavior of the PMT base is preserved, the high-frequency bypass capacitors in the base are located in the

upstream part, mounted very close to the socket pins. The upstream and downstream base components are separated by a flexible partition which separates the air volume into two regions. In the electronics region circulating chilled air is used to control the temperature of the readout electronics. In the upstream region, a relatively stationary air volume is separately temperature controlled to maintain the temperature of the array. All regions of the CsI house are maintained at a relative humidity of less than 2%.

1.1.5. Calibration and Monitoring

The stringent energy resolution requirements and the relative complexity of the DPMT readout technology make calibration a formidable task. Because the readout chip operates with four integration capacitors for each of nine independent ranges, and each capacitor has an independent slope and offset when presented to the digitizer, the calibration of a single channel requires the determination of 72 independent constants. In addition, the photomultiplier response will be slightly non-linear over the operational dynamic range. In order to calibrate the electronics, a laser flasher system will be used. The flasher uses a YAG laser to excite a light flash in a fluorescent dye. This light flash is viewed by several PIN photodiodes which are used to measure the light level, and by 3100 quartz optical fibers which carry the light pulse to the individual crystals. A fiber brings the light to the rear of a crystal and the light must reflect off the front face to arrive back at the photomultiplier. Since all of the PMT's and PIN diodes view the same light flash, all of these devices should track. By varying the intensity of the original laser flash, the PMT/digitizer response can be calibrated against the PIN diode response over the entire dynamic range of the system. The PIN diode signals are digitized using a 20-bit Burr Brown ADC, and the combination has been shown to be linear to 0.1% over the range required for KTeV calibration[5]. Since the flasher system passes light through the crystal and drives the entire signal processing chain, it is sensitive to any changes in the behavior of the calorimeter.

Another crucial monitoring issue is crystal quality. Although it is expected that radiation

damage will not be significant, it is important to monitor for the onset of problems. The most sensitive measure of damage is a change in the longitudinal response of the crystals, and this will be continuously measured using a cosmic ray telescope. Scintillation counters above and below the array will be used to trigger on and track cosmic ray muons which pass vertically through the crystals. A 1 m thick iron range stack below the array will ensure that the muons have a minimum momentum to reduce multiple scattering. Using this technique, the relative longitudinal response of each crystal will be determined to 2% accuracy every three days.

1.1.6. Test Beam Results

To verify the performance of the KTeV CsI calorimeter, a 5×5 test array was constructed from twenty-five 5 cm square production crystals. This array was instrumented with production photomultipliers and prototype readout electronics, and was tested in the X1 Test Beam facility at the CERN SPS. In the test, the calorimeter was exposed to electron beams of fixed momenta of 5, 10, 20, 30, 40, and 60 GeV/c. Other runs were taken using 20 and 40 GeV/c π^- , 40 GeV/c π^+ , and 70 GeV/c muons. The muon runs were taken with the detector oriented perpendicular to the beam, and were used to verify the longitudinal uniformity of the crystal response. Figure 4 shows a preliminary analysis of the electron data. In each case the data in the central peak has been fitted to a gaussian. Figure 5 shows the resulting gaussian widths as a function of the beam momentum, compared to the Monte Carlo prediction for the resolution. The contribution to the gaussian width from the momentum spread of the beam is included in the Monte Carlo. From the figure it can be seen that the measured resolutions satisfy the requirements of the experiment even before the beam momentum spread is taken into account.

1.2. The E-731 Lead Glass Array

The E-731 lead glass calorimeter has been described extensively in a number of PhD dissertations[12] and was used in E-731 to search for direct CP-violation. More recently the E-731 ap-

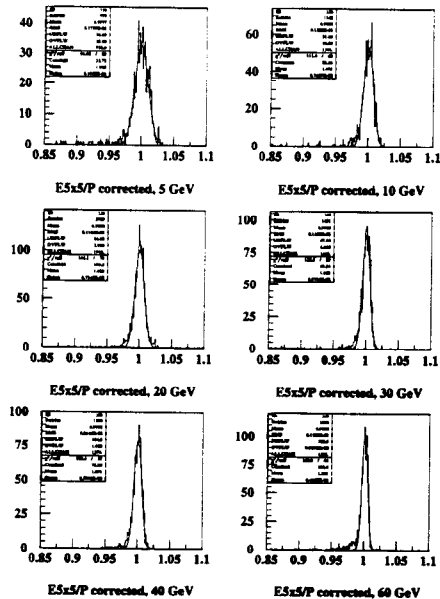


Figure 4. Preliminary electron resolution data taken with a sample of the KTeV CsI array.

paratus or rearrangements of it has been used to search for CPT violation in E-733, and to study rare decays of the K_L^0 in E-799. The array, shown in Figure 6, consisted of 804 blocks of Schott F-2 lead glass stacked in a circular array with two holes near the center to allow two neutral kaon beams to pass through. Each $5.8 \times 5.8 \times 60.2 \text{ cm}^3$ block was wrapped in 0.0005 in thick aluminized mylar, and was instrumented with a phototube which was pressure mounted to the back. The phototube was separated from the glass by a silicon gel cookie which had an index of refraction between that of the lead glass and that of the PMT glass. Inside the gel wafer a Wratten 2A filter was embedded to improve the attenuation length of the glass. The energy resolution of this device is $2.5\% + 5\%/\sqrt{E}$ for photons.

Because its resolution and radiation hardness are inadequate for the next generation of high rate and high precision kaon experiments, the E-731 array will be replaced by the new KTeV CsI calorimeter. In the next fixed target run, the E-

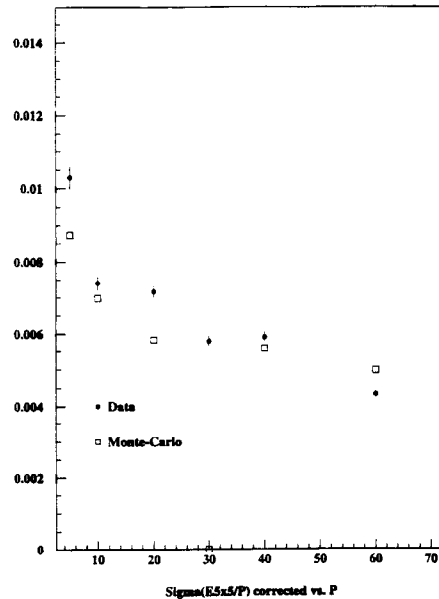


Figure 5. Preliminary measurements of the KTeV energy resolution as a function of beam momentum.

731 array will be reconfigured to serve as the electromagnetic calorimeter for the E-832 photoproduction experiment, which will be discussed in a later section.

1.3. The E-705 Scintillating Glass Array

The E-705 experiment[6] was designed to study direct photon production in the interactions of $300 \text{ GeV}/c$ hadrons with a lithium target, and to reconstruct the radiative decays of the $\chi_1(3510)$ and $\chi_2(3555)$ states of charmonium. Both of these physics goals placed demanding requirements on the performance of the photon detector. In particular, the radiative decay $\chi \rightarrow J/\psi(3097) + \gamma$ required excellent energy resolution for photons down to $2 \text{ GeV}/c^2$ and that the acceptance of the detector be very large to detect soft wide angle photons. At high energy, the direct photon measurement drove the specifications requiring linear response up to $200 \text{ GeV}/c^2$ and sufficient position resolution to distinguish

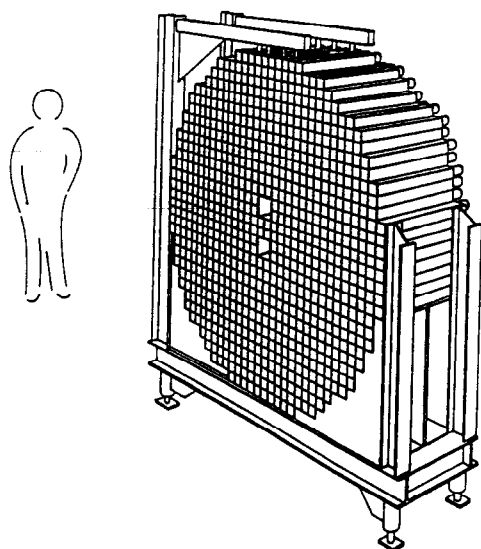


Figure 6. The E-731 lead glass array.

high energy single photons from π^0 's. Since unmatched photons from the decay $\pi^0 \rightarrow \gamma\gamma$ are a significant background both for radiative decays and direct photons, a large acceptance was also important for detecting wide angle photons from π^0 decay. To balance between the sometimes conflicting goals of energy and position resolution, cost, and radiation hardness, a hybrid device was constructed. The E-705 electromagnetic calorimeter consists of an array of scintillating glass blocks near the beam and lead glass blocks on the outer perimeter. The array is preceded by preshower detectors consisting of a lead/gas tube sampling device near the beam region and scintillating glass active converters followed by gas tube hodoscopes in the outer part of the array. The device is described in detail in the literature[7], so only the salient features will be repeated here.

1.3.1. Mechanical Details

Figure 7 shows the E-705 electromagnetic calorimeter in plan view (above) and in beam's eye view. The Main Array is 375 cm by 195 cm with a 30 cm by 15 cm beam hole in the cen-

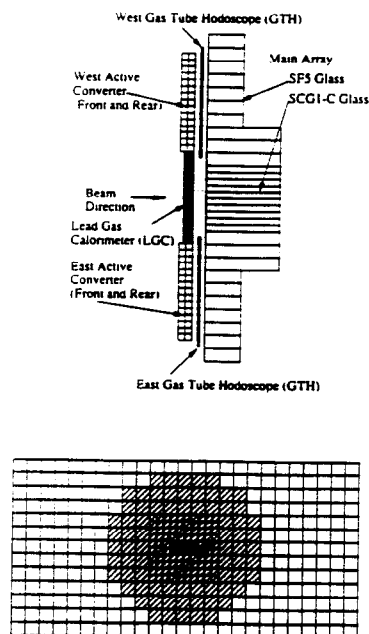


Figure 7. Plan view and beam's eye view of the E-705 Electromagnetic calorimeter.

ter and consists of three types of blocks. Near the beam region are $7.5 \times 7.5 \times 89 \text{ cm}^3$ blocks of SCG1-C scintillating glass 20.9 radiation lengths deep. The middle annular region used similar blocks with a $15 \times 15 \text{ cm}^2$ cross section. Scintillating glass blocks were chosen for the central region because they are about 150 times more radiation hard than lead glass. The outer part of the array was constructed from $15 \times 15 \times 41.5 \text{ cm}^3$ blocks of SF5 lead glass.

The Active Converters were formed from $7.5 \times 7.5 \times 97.5 \text{ cm}^3$ SCG1-C blocks arranged in columns two blocks high and two blocks deep. These blocks serve as preshower detectors in the region in front of the lead glass. Following the active converters is a gas tube hodoscope which enhances the shower position resolution of the calorimeter. This device consists of two planes of vertical rectangular polystyrene tubes each having a 50 micron gold-plated tungsten wire down its center. The cell size for this device is 0.88 cm

near the center of the array and 1.76 *cm* to the outside. The two planes were separated by a copper clad G-10 ground plane and were sandwiched between circuit boards etched with horizontal strips. The wires and cathode pad strips provided horizontal and vertical shower position information, respectively.

In the beam region the position resolution comes from the lead-gas calorimeter. This device also reads out the shower position with vertical wires and horizontal pads, but here there are no preconverter blocks. Instead, the particles first encounter 1.3 *cm* of steel, 0.8 *cm* of lead, and then 8 layers of gas tube planes alternating with 0.12 *cm* Pb plates.

1.3.2. Performance Results

Because of the geometric complexity of the E-705 calorimeter, the resolution is also complicated. The fractional energy resolution $\sigma(E)/E$ was measured in calibration beams to be $(1.71 \pm 0.10\%) + (11.83 \pm 0.43\%)/\sqrt{E}$ in the SCG1-C scintillating glass with the lead-gas preconverter, $(0.990 \pm 0.056\%) + (4.58 \pm 0.22\%)/\sqrt{E}$ in the SCG1-C scintillating glass with the SCG1-C active converter, and $(0.331 \pm 0.018\%) + (6.65 \pm 0.08\%)/\sqrt{E}$ in the SF5 lead glass with the SCG1-C active converter. The position resolutions ranged from 2 to 6 *mm* for all regions of the calorimeter.

Perhaps the best measure of the performance of the device is its ability to reconstruct events from the decay $\chi \rightarrow J/\psi(3097) + \gamma$. Figure 8 shows the χ signals obtained by E-705 using pion and proton beams. Although clearly near the limits of resolution, the experiment was able to separate the χ_1 and χ_2 peaks to make this analysis.

1.3.3. Status

The E-705 Experiment is now complete and is being decommissioned. The array of scintillating glass and lead glass blocks will be reconfigured to serve as the electromagnetic calorimeter for a new proton beam dump experiment, E-872, designed to make a direct observation of the ν_τ . E-872 is currently under construction.

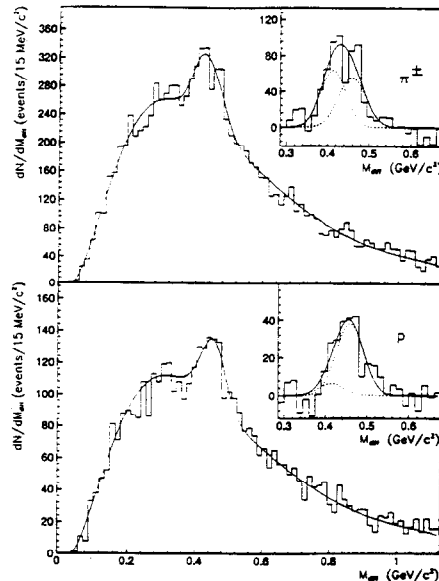


Figure 8. Signals for χ states reconstructed in the E-705 pion beam and proton beam data.

1.4. The E-760 Pb-glass Barrel

The E-760 experiment was also designed to study the χ states, but uses a very different strategy from E-705. E-760 is located in the Fermilab Antiproton Accumulator, and uses an internal gas jet target to create proton antiproton collisions. The calorimetry requirements are quite relaxed here compared to traditional fixed target experiments, because the calorimeter must serve only to identify the correct event topology and separate events from background. The antiprotons are initially captured at an energy above that required to produce χ states in collisions with stationary protons, and are *decelerated* in order to scan through the χ resonances. The energy measurement is obtained from the energy of the antiproton beam. In the antiproton accumulator, a beam of up to 4×10^{11} circulating \bar{p} 's is cooled to $\delta p/p = 2 \times 10^{-4}$ allowing the sub-MeV widths of the charmonium states to be measured directly.

1.4.1. Mechanical Details

The E-760 apparatus, shown in Figure 9, consists of a cylindrical array of 1280 lead glass blocks tapered and oriented to point back to the $p\bar{p}$ interaction point. A planar electromagnetic calorime-

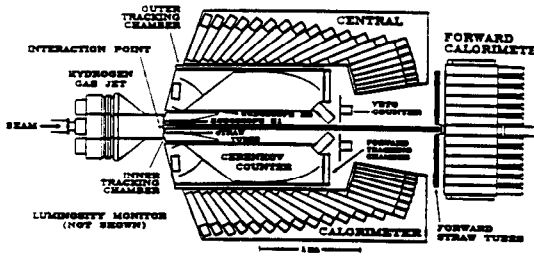


Figure 9. The E-760 apparatus

ter covers the forward direction, and inside are hodoscopes, tracking chambers, and a Cerenkov counter to aid in electron identification. The lead glass calorimeter[8] covers 360° in azimuth and 10° to 70° in polar angle. The calorimeter was divided into 64 equal wedges in ϕ . Each wedge is a mechanically independent assembly consisting of 0.735 mm thick stainless steel skins, connected by 0.254 mm fins which separate the blocks as shown in Figure 10. One wedge assembly contains twenty lead glass blocks. The individual blocks were made from F2 lead glass and instrumented with photomultiplier tubes which are glued to the blocks. The blocks are wrapped in a thin white paper cushion and are fit into the pockets in the wedge assembly. The wedge assemblies then fit together to form the cylindrical calorimeter.

1.4.2. Performance

The performance of the E-760 calorimeter has been studied at the Medium Energy Separated Beam (MESB-B2) at BNL. The best energy resolution was found to be $\sigma(E)/E = 3\%/\sqrt{E}$, and the average energy resolution was $\sigma(E)/E = (3 \pm 0.3)\%/\sqrt{E} + (1.5 \pm 0.5)\%$. Because of the energy loss in the steel partitions between wedges, the energy resolution is degraded to $8\%/\sqrt{E}$ over

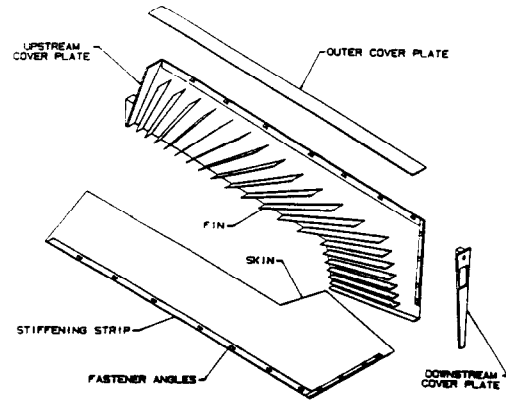


Figure 10. The wedge assembly used on the E-760 lead glass calorimeter

a small region near the crack. Although the energy resolution of the calorimeter is modest, the ultimate power of the apparatus comes from the precisely determined machine energy. Figure 11 shows the χ_1 and χ_2 states as measured by E-760. The states are very clearly resolved and precision measurements of the χ_1 and χ_2 line parameters have been published[9].

2. LIQUID ARGON CALORIMETRY

2.1. The E-706 Liquid Argon Calorimeter

The primary physics goal of E-706 was the study of direct photon production in proton and pion interactions. As a secondary physics goal and an important measurement for understanding the backgrounds to direct photons, E-706 also performed detailed measurements of the neutral pion production cross-sections. To perform these measurements, the E-706 collaboration chose to construct a lead/liquid argon electromagnetic calorimeter (LAC). It is interesting to contrast this device with the E-705 apparatus which was also aimed at direct photon studies, but which had the additional goal of studying the radiative decays of the χ states. It was the need for excellent energy and position resolution for photons with energy as low as $2 \text{ GeV}/c^2$ that drove the E-705 design to a rather complicated detector with

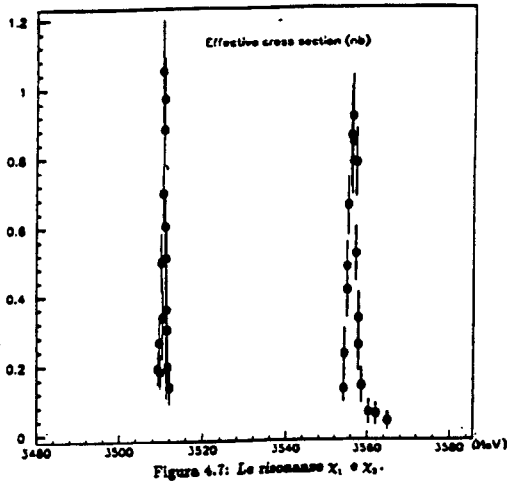


Figure 11. The χ_1 and χ_2 states, as measured by E-760.

four distinct regions each having different energy and position resolution. While this accomplished the goals of resolving the χ states, the resulting calibration complexity makes the study of direct photons rather more difficult. Here the physics requires the analysis of rapidly falling photon energy spectra, and having a uniform, well understood energy response and resolution for photons and electrons is the crucial issue. Because the E-706 apparatus is optimized only for these relatively high P_{\perp} processes, a device with relatively poorer low energy photon response was acceptable. The E-706 LAC is a geometrically simple device consisting of circuit boards etched with r and ϕ measuring pads alternating with lead plates suspended in a liquid argon cryostat as shown in Figure 12. The active area of the device is 160 cm in radius with a 20 cm beam hole in the center. The details of the construction and calibration of this device have been described elsewhere[10, 11] so only a very brief outline of the calibration process will be repeated here. The E-706 $\gamma\gamma$ data show very prominent π^0 and η peaks. An analysis of the ratio of the measured invariant masses to the nominal values for these particles shows 3% radial variation in the calorimeter response from

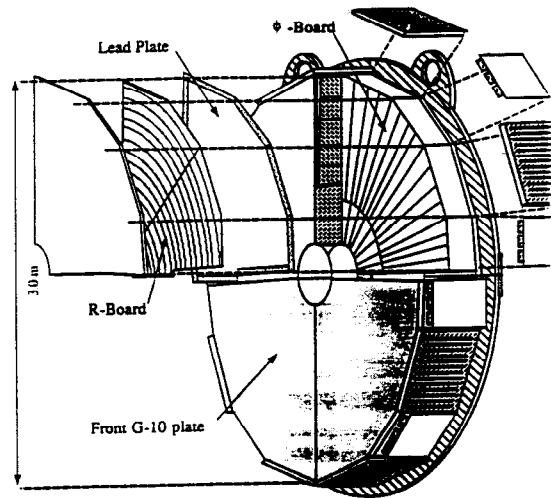


Figure 12. Construction of the E-706 liquid argon EM calorimeter.

the inside edge to the outside. The variation is the same for both the π^0 and η peaks. Using the π^0 ratio as a correction factor, the ratio of the η peak to the nominal η mass can be used as a check. This analysis is shown in Figure 13. The relative response of the LAC to electrons and photons was also a critical issue, and a detailed Monte Carlo simulation was necessary make this determination. An elegant demonstration of the net result of the calibration efforts is provided by an analysis of the Dalitz decays of the π^0 and η . Figure 14 shows the $\gamma e^+ e^-$ invariant mass peaks in the vicinity of the π^0 and η . The lower plot shows the ratio of the measured $\gamma e^+ e^-$ invariant mass to the nominal π^0 or η mass as a function of photon energy. The flatness of this plot shows that the relative response of electrons and photons is understood over the entire dynamic range of the device.

3. THE E-831 EXPERIMENT

The physics objective of the E-831 is to study the photoproduction and decay of charm particles. The experiment is located in Fermilab's

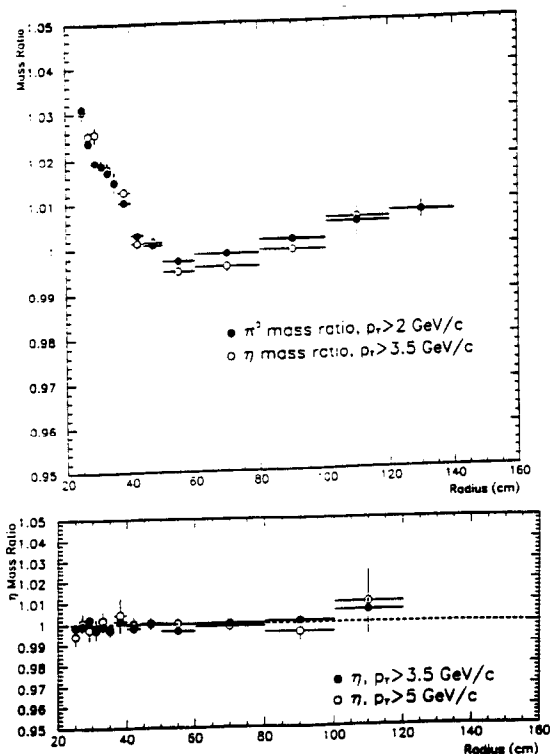


Figure 13. Radial variation of the E-706 LAC response, and a verification of the correction algorithm (lower plot).

Wide Band Photon Beam[13], and is a continuation of the earlier E-687 effort which accumulated 10^5 charm events. The new experiment will use an upgraded detector which will operate at five times the average luminosity of the previous experiment. An upgraded triggering and data acquisition experiment will accumulate data at double the earlier rate. The goal of E-832 is 10^6 fully reconstructed charm particles.

The basic layout of the E-687/E-831 spectrometer[14] is shown in Figure 15. The apparatus is a two magnet spectrometer using an 8,400 channel silicon microstrip detector and 13,400 wires of proportional chambers for tracking. Three multi-cell Cerenkov counters provide particle identification. Two electromagnetic calorimeters are

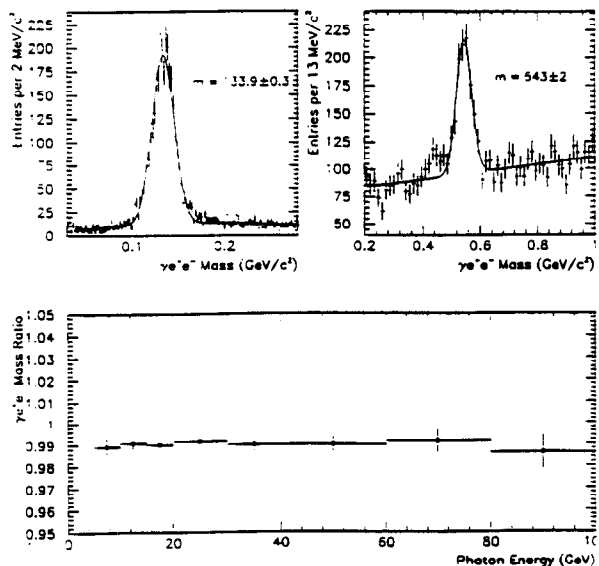


Figure 14. Dalitz invariant mass plots (above), and the mass ratio (below).

used. One is a conventional lead/plastic scintillator shower counter arranged midway down the spectrometer to detect wide angle tracks. The other electromagnetic detector covers the forward direction and is located at the downstream end of the experiment. The forward EM calorimeter is followed by a hadron calorimeter and a muon detector. It is the forward calorimetry which must be upgraded to accommodate the increased luminosity.

3.0.1. The Forward EM Calorimeter

The E-687/E-831 collaboration has used a number of different devices and technologies for forward electromagnetic calorimetry during the course of their experimental program. The original device was a $255\text{ cm} \times 205\text{ cm}$ conventional Pb/scintillator shower counter constructed from strips of plastic scintillator ganged together with light guides and read out with photomultipliers. The strips were arranged to provide fine lateral and longitudinal segmentation. The original device was destroyed by fire in October, 1987.

mits the converted light. The wavelength shifting fiber is spliced to a clear fiber which carries the shifted scintillation light out to the edge of the device. The routing of the clear fibers is accomplished in a separate plastic layer which backs up the scintillator layer. The fibers pass out of the groove in the scintillator and into a groove in the backing layer. The complicated paths indicated in the routing panel serve to equalize the path lengths of fibers so that all signals arrive at the calorimeter edge at the same time. In front of the scintillator layer is another passive plastic layer which is routed with grooves containing metal tubes through which a radioactive source can be passed on a wire to calibrate individual tiles. The package is squeezed between a rib and gusset support panel on the front and a solid cover plate on the back. A spongy compressible layer serves to hold the entire package firmly together. The clear fibers from each tower are ganged together at the edges of the calorimeter and routed to photomultiplier tubes.

4. The Liquid Scintillator Calorimetry

4.1. The TPL Calorimeter

The Tagged Photon Laboratory (TPL) at Fermilab has been the site of a series of heavy flavor experiments. E-691, which completed data-taking in 1985, studied charm production in $\gamma - Nucleus$ collisions. During the 1987-88 fixed target run, E-769 used the TPL spectrometer to study the flavor, x , p_{\perp} , and A dependence of charm hadroproduction. In the 1991 run, E-791 used the TPL spectrometer with a $500 GeV/c \pi^-$ beam to accumulate 200,000 charm decay events. The TPL spectrometer uses silicon microstrips for vertex detection, two analysis magnets and drift chambers for tracking, and Cerenkov counters for particle ID. The downstream calorimetry consists of a segmented liquid scintillation calorimeter (SLIC) followed by a hadron calorimeter and muon wall. The downstream calorimeters are shown in Figure 17. The hadron calorimeter is conventional Fe/scintillator sampling device consisting of 36 layers of 2.5 cm thick steel plate. Each plate is 2.7 m high and 4.9 m wide. The gaps are instrumented with orthogonal 14.3 cm

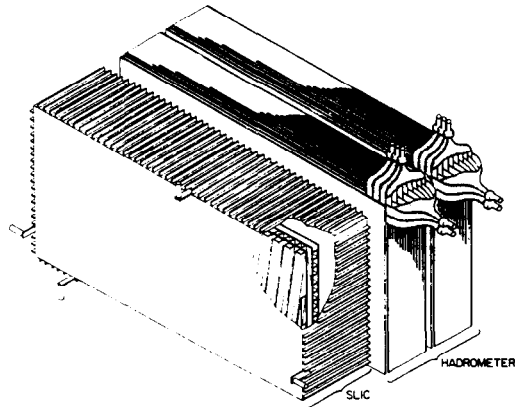


Figure 17. The Tagged Photon Laboratory electromagnetic and hadronic calorimeters.

strips of x and y counters made from acrylic scintillator. The performance of the device is canonical, having a hadronic energy resolution $\sigma(E)/E = 75\%/\sqrt{E}$. The SLIC is a more interesting device which is formed from teflon coated sheets of corrugated aluminum. The corrugated layers are alternated with flat layers of teflon coated lead forming a lead scintillator structure in which the scintillation layer is divided into isolated cells by the corrugations. The scintillation layer is filled with a mineral oil based liquid scintillator, and the teflon coatings on the plates provide total internal reflection. The corrugations are arranged in a repeating U, V, Y pattern for a total of 60 layers. The Pb plate amounts to $1/3$ of a radiation length per layer. The ends of the sampling layers are ganged together in Z using wavelength shifter bars which are connected to photomultipliers for readout. The result is a simple, robust device with energy resolution of $12\%/\sqrt{E}$ and position resolution of 3 mm over a dynamic range from $0.1 GeV/c$ to $100 GeV/c$. The SLIC was described in the literature in 1984[16], and the TPL collaboration has monitored its performance carefully over the years. The performance of the device has not degraded significantly over ten years, although the relative muon to electron response has shifted about 20%, consistent with a

degradation of the attenuation length of the wavelength shifter bars.

4.2. The Lab E Neutrino Calorimeter

The Lab E Neutrino detector has been in operation for a number of years and has been used to study nucleon structure functions, neutrino oscillations and other topics in neutrino physics. Two runs using a quadrupole triplet beam (E-744 in 1985, and E-770 in 1987-88) accumulated a total of approximately 3.6 million charged current and 1.1 million neutral current events. In the next fixed target run, E-815 will use this apparatus to perform a precision measurement of $\sin^2\theta_W$. As a calorimeter, the Lab E detector is not very interesting[17]. The basic unit of the calorimeter is a $10 \times 10 \text{ ft}^2 \times 4 \text{ in}$ thick Fe plate followed by a $10 \times 10 \text{ ft}^2$ unsegmented scintillation counter. This basic unit repeats up to a total mass of 690 tons. The counters consist of a ten foot square by one inch thick clear plastic tanks, supported internally by ribs every inch. The tank is filled with Bicron BC-210 liquid scintillator. Wavelength shifter bars along the edges convert the scintillation light and guide it to photomultipliers at each corner. The resolution of the device, $\sigma/E = 0.89/\sqrt{E}$, is dominated by the sampling frequency.

Studies of the counter performance indicate that over the past ten years, the liquid scintillator light output has degraded by a factor of two. It is suspected that contamination from brass valves is the cause of the degradation[17]. To upgrade the device for the 1996 run, the 1650 l of liquid scintillator has been replaced, and the brass valves have been replaced by teflon valves.

5. PLASTIC SCINTILLATOR DEVICES

5.1. The E-605 Calorimeter

The E-605 apparatus, first constructed in the early 1980's to study dimuon production, has since been used for a number of dimuon experiments and has been used to search for two-body decays of the B mesons. The apparatus is a strongly focussing spectrometer with a very narrow acceptance for two particle final states in which two oppositely charged tracks emerge back

to back at 90° relative to the beam direction in the center-of-mass frame. A second magnet and drift chambers are used to reconstruct the momenta of the two tracks, and a large ring-imaging Cerenkov counter is used for particle identification. The event reconstruction is done with the tracking system and calorimetry is primarily used for triggering. The requirements on the calorimeter are therefore not very demanding. The E-605 calorimeter, shown in Figure 18, consists of a con-

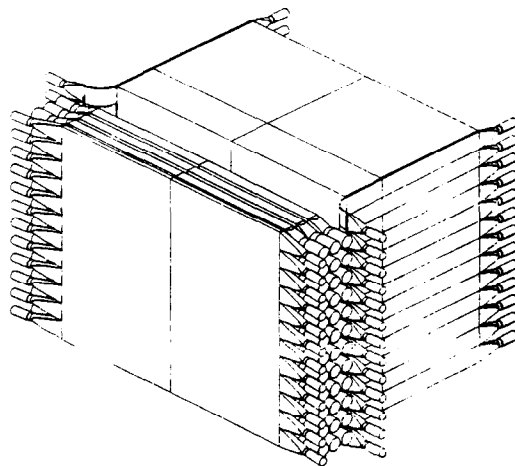


Figure 18. The E-605 electromagnetic and hadronic calorimeters.

ventional hodoscopic lead scintillator electromagnetic section, and an iron scintillator hadronic section which is read out using wavelenght bars which gang scintillators in Z .

5.2. The E-683 Jet Calorimeter

The physics goal of E-683 was to study the photoproduction of high- p_\perp hadron jets. The calorimeter used in E-683 was originally constructed for an earlier experiment, E-609, which studied high- p_\perp hadron jet production in proton-nucleus collisions. The crucial calorimeter design requirement for studying high- p_\perp phenomena is uniformity. Because the production spectrum for large transverse momentum jets falls very steeply,

the measured spectrum is affected by the resolution. In particular, any high-side tail in the response will have a profound influence on the measured spectra. The E-683 calorimeter was designed to provide a very uniform response, free from "hot spots" over its entire active area. The calorimeter, shown in Figure 19, is constructed

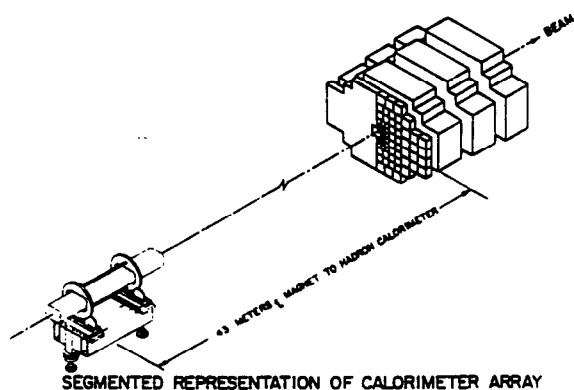


Figure 19. The E-609/E-683 calorimeter.

from 528 individual modules stacked to form 132 longitudinal towers each four modules deep. The modules grow larger in successive layers to preserve the tower structure, pointing back to the interaction point. Each module is a self contained calorimeter unit consisting of a stack of square absorber plates instrumented with plastic scintillators. Each scintillator is split along its diagonal where a wavelength shifter converts the light and guides it to the corner. The wavelength shifter bars from each tile are ganged together into a photomultiplier tube using individual lucite light guides. Paint applied the light guides was used to equalize the response of each scintillator. Because the photomultipliers in this calorimeter are located *inside* the array, there is a possibility of large amounts of Cerenkov light being created by particles passing through the glass of the PMT envelope. To avoid this problem the designers developed a special PMT which employed a spe-

cial photocathode on a mica wafer separated from the PMT glass. The E-683/E-609 calorimeter is described in detail in a 1983 Master Thesis[18].

REFERENCES

- 1 KTeV Design Report, Fermilab Publication FN-580, January, 1992.
- 2 L.K. Gibbons et al., Phys. Rev. Lett. 70 (1993) 1199.
- 3 H. Kobayashi et al., KUNS-900, 1987.
- 4 R.J. Yarema et al., Fermilab Conf-92/148, May, 1992.
- 5 S. Hansen and H. Nguyen, private communication.
- 6 Antoniazzi et al., Phys. Rev. D46 (1992) 4828, and Antoniazzi et al., Phys. Rev. Lett. 70(1993) 487.
- 7 Antoniazzi et al., Nucl. Instr. and Meth. A332 (1993) 55-57.
- 8 Bartoszek et al., submitted to Nucl. Instr. and Meth.
- 9 Armstrong et al., Nucl. Phys. B373, 35 (1992).
- 10 W.E. DeSoi, PhD Thesis (University of Rochester, 1990), F. Lobkowicz et al., Nucl. Instr. and Meth. A235 (1985), 332.
- 11 N. Varelas, PhD Thesis (University of Rochester, 1994).
- 12 J.R. Patterson, PhD Thesis (University of Chicago, 1990), L.K. Gibbons, PhD Thesis (University of Chicago, 1993).
- 13 J. Butler et al., Fermilab TM963, April, 1980.
- 14 P.L. Frabetti et al., submitted to Nucl. Instr. and Meth.
- 15 John Cumulat, private communication.
- 16 V.K. Bharadwaj et al., Nucl. Inst. and Meth. 228 (1985) 283, and J.A. Appel et al., Nucl. Inst. and Meth. A243 (1986) 361.
- 17 R. Bernstein, private communication.
- 18 K.A. Johns, Masters Thesis (Rice UNiversity, 1983).